AD 276 699

RADC-TDR-61-190

See title page

(10)

October 1961

TIME DOMAIN ANTENNA TECHNIQUES

Technical Note

Approved:
W. H. Kummer
Project Manager, Time Domain Antenna Techniques
Antenna Department
Research and Development Division
Hughes Aircraft Company
Culver City, California

P61-22
Contract AF 30(602)-2410

Prepared For

ROME AIR DEVELOPMENT CENTER
AIR FORCE SYSTEMS COMMAND
UNITED STATES AIR FORCE
GRIFFISS AIR FORCE BASE
NEW YORK

RADC-TN-61-290 October 1961

TIME DOMAIN ANTENNA TECHNIQUES

Technical Note

Approved:

W. H. Kummer
Project Manager, Time Domain Antenna Techniques
Antenna Department
Research and Development Division
Hughes Aircraft Company
Culver City, California

P61-22

Contract AF 30(602)-2410
Project No. 4506
Task No. 450604

Prepared For

ROME AIR DEVELOPMENT CENTER
AIR FORCE SYSTEMS COMMAND
UNITED STATES AIR FORCE

GRIFFISS AIR FORCE BASE
NEW YORK

FOREWORD

This report has been written by the following personnel:

T.S. Fong

F.G. Terrio

W.H. Kummer

A.T. Villeneuve

In addition, the assistance of the following persons is acknowledged:

E.D. Shaw

O.C.L. Witte

ABSTRACT

This report concerns the application of time modulation of array antennas to the problems of obtaining ultra-low sidelobe and simultaneously scanned antenna patterns.

A design analysis is presented for a linear array which obtains reduced sidelobe levels by on-off switching of the individual array elements and subsequent filtering of the array output signal. A simplified experimental array design is presented, and the switching circuitry developed for this ultra-low sidelobe array is also described.

Stable transmitting and receiving equipment, designed for time domain applications, is discussed and performance characteristics of the equipment are given.

The final results of the tests of the antenna pattern range are presented. Measurements to determine the repeatability of low sidelobe patterns are discussed. It is concluded that 40 db sidelobes can be measured to within ±1.5 db on the present range.

The basic theory of the technique of Simultaneous Scan is given. An experimental array and its required control circuitry are under development.

CONTENTS

INTRODUCTION

The use of time as a fourth dimension in obtaining improved antenna performance was proposed in an article published several years ago, and the possible applications of these time domain antennas were discussed therein. Among the applications mentioned were sidelobe suppression and simultaneous scan.

Since that time considerable study has been directed toward showing the feasibility of the sidelobe suppression technique and many facets of the problem have been considered by Hughes Aircraft Company.

This report discusses the work now in progress which represents an extension of the above mentioned sidelobe suppression studies, as well as a study of the feasibility of applying the technique of simultaneous scan to a typical radar system.

This technical note covers the progress made since the publication of Report No. RADC-TN-61-145. The studies in that report indicate that a reduction of sidelobes by time domain techniques is best obtained by using a single array with on-off switching of elements rather than by combining the outputs of two side-by-side arrays.

In the present report a design theory for determining the element on-off times for arrays of switched radiators which are shunt coupled to a main feedline is presented. Based on this design study, an array, including switch programming circuitry, is under construction and will be tested when the required stable transmitter and receiver are completed. The stability requirements of the transmitter and receiver result from the fact that the time domain systems require a receiver with a local oscillator which is coherent with the transmitter signal at least over the time required to process, i.e., filter and record the received signal. The required transmitter and receiver are being constructed and are nearing completion. The designs of the transmitter, receiver, and other components which constitute the circuitry for the sidelobe suppression system are also discussed.

The tests of the pattern range have continued with emphasis on the effects of reflections emanating from the region near the receiving

antenna. A series of patterns of an existing array has been taken for various orientations of the array and shows results repeatable in essential detail to levels 40 db below the main peak except in the region ±45 degrees off the main beam. The reasons for these deviations in the patterns are discussed. It is concluded that the range is adequate for measurement of sidelobes down to 40 db below the main beam.

The basic principles of the technique of simultaneous scan are presented. The technique consists of the sequential on-off switching of the elements of a linear array in a periodic fashion. The signal resulting from combining the outputs in a single channel is a phase-modulated signal containing the direction of arrival information. By filtering the spectral components introduced by the modulation, conventional array patterns with different beam pointing directions are produced. An experimental twenty-element array has been designed and is presently under construction.

DISCUSSION

DESIGN OF SINGLE LINEAR ARRAY WITH SWITCHING TO OBTAIN SIDELOBE SUPPRESSION

Previous analyses[1,2] and the analysis of Technical Note RADC-TN-61-145 have shown that mechanical tolerances in cutting slots, and the mutual coupling between elements in the array are the main problems in low sidelobe array design. Also, an error analysis of on-off switched broadwall shunt slots indicates that switching can reduce the effects of excitation errors. Therefore, this section contains a theoretical design study of a linear array of shunt-coupled slots in which switching is used to obtain reduced sidelobes. The effects of impedance changes resulting from the switching are considered and a simplified experimental array which circumvents these changes in impedance is also discussed.

Design Analysis

Consider a linear array of uniformly spaced radiators which are shunt-coupled to a main feed transmission line, as in Figure 1. Each element is to be controlled by an on-off r-f switch which effectively couples and decouples the element to the main line. All switches are assumed to be identical and to be matched and lossless when on, and perfectly reflecting when off. The on-off switching is used to obtain additional control of the aperture distribution so that low sidelobe patterns may be obtained.

In the first part of the analysis various relations between admittances and the equivalent voltages developed in the antenna are derived. This is done in order to obtain a relation between conductances of the array and the coefficients of the static aperture distribution. From their relation it is possible to determine the required on times of the elements of the array which will give a certain amount of sidelobe suppression.

The array will be designed for use as a receiving array. However, reciprocity[3] allows the use of the transmitting characteristics of the array in the design. Let $\mathcal{G}(\theta, \phi)$ denote the gain of the antenna as

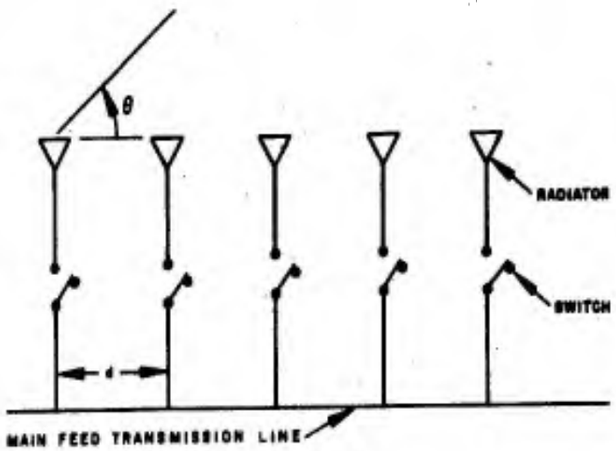

Figure 1.

determined from transmitting characteristics and G_{in} represent the input conductance of the antenna (assumed resonant). On receive, the antenna can be represented by an equivalent generator of internal admittance G_{in} and of open circuit voltage given by[3]

$$V = \lambda\sqrt{\frac{2}{\pi G_{in}}\,\mathcal{D}(\theta,\phi)}\,\exp(j\zeta)\sqrt{S_i}\,\exp(j\psi) \qquad (1)$$

where λ is the wavelength of incident radiation, S_i is the incident power density (plane wave assumed) and ζ and ψ are phase functions of the field intensity of the transmitting pattern and of the incident field respectively.

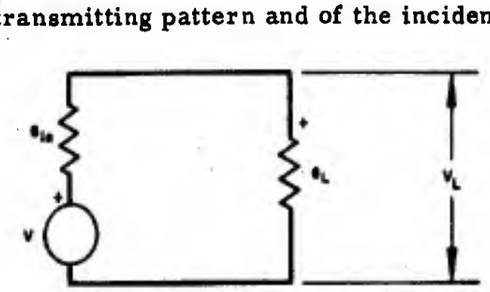

Figure 2.

Thus, from Figure 2 the signal across the load, G_L, is given by

$$V_L = \frac{G_{in}}{G_L + G_{in}} V = \lambda \sqrt{\frac{2}{\pi}} \frac{\sqrt{G_{in}}}{G_L + G_{in}} \sqrt{\mathcal{D}(\theta, \phi)} \exp(j\zeta) \sqrt{S_i} \exp(j\psi) \qquad (2)$$

For the type of array under consideration here the field pattern is given by[3]

$$f(\theta, \phi) = e(\theta, \phi) \sum_{n=0}^{N-1} b_n \exp(jknd\cos\theta) \qquad (3)$$

where the b_n are the relative excitation coefficients of the array elements and $e(\theta,\phi)$ is the element factor. The gain of an antenna is related to the field pattern by

$$\mathcal{D}(\theta, \phi) = \frac{4\pi f(\theta, \phi) f^*(\theta, \phi)}{\iint_{\text{sphere}} f(\theta, \phi) f^*(\theta, \phi) \, d\Omega} \qquad (4)$$

Therefore, one may write

$$\left[\mathcal{D}(\theta, \phi)\right]^{1/2} \exp(j\zeta) = \frac{2\sqrt{\pi}\, e(\theta, \phi) \sum_{n=0}^{N-1} b_n \exp(jknd\cos\theta)}{\left(\sum_{n=0}^{N-1} \sum_{p=0}^{N-1} b_n b_p^* I_{np} \right)^{1/2}} \qquad (5)$$

where

$$I_{np} \equiv \iint_{\text{sphere}} |e(\theta, \phi)|^2 \exp\left[jk(n-p)d\cos\theta\right] \sin\theta \, d\theta \, d\phi \qquad (6)$$

It is now necessary to relate the b_n to the array parameters. For this purpose it is assumed that the elements are endplate waveguide slots and that they are fed through branch waveguides containing microwave switches. The branch guides are coupled to the main feed waveguide at $\lambda_g/2$ intervals through resonant displaced longitudinal shunt slots in the feed guide. Adjacent slots are offset on opposite sides of the feed guide axis to compensate for the phase reversals which occur in the feed guide at $\lambda_g/2$ intervals. For these conditions it may be shown that[4, 5]

$$b_n \propto \sqrt{G_n} \tag{7}$$

where G_n is the effective conductance that the nth branch line presents to the main feed line; Equation 5 becomes

$$\left[\mathcal{D}(\theta, \phi)\right]^{1/2} \exp(j\zeta) = \frac{2\sqrt{\pi}\, e(\theta, \phi) \sum_{o}^{N-1} \sqrt{G_n} \exp(jknd\cos\theta)}{\left(\sum_{o}^{N-1} \sum_{o}^{N-1} \sqrt{G_m G_p}\ I_{mp}\right)^{1/2}} \tag{8}$$

and the received voltage per unit incident field intensity may be written

$$v_L = \frac{V_L}{\sqrt{S_i}\exp(j\psi)} = \lambda\sqrt{\frac{2}{\pi}} \frac{\sqrt{\sum_{o}^{n-1} G_q}}{\left(G_L + \sum_{o}^{N-1} G_q\right)} \frac{2\sqrt{\pi}\, e(\theta, \phi) \sum_{o}^{N-1} \sqrt{G_n} \exp(jknd\cos\theta)}{\left(\sum_{o}^{N-1} \sum_{o}^{N-1} \sqrt{G_m G_p}\ I_{mp}\right)^{1/2}} \tag{9}$$

The term

$$\frac{\sqrt{\sum_{o}^{n-1} G_q}}{\left(\sum_{o}^{N-1} \sum_{o}^{N-1} \sqrt{G_m G_p}\ I_{mp}\right)^{1/2}} \tag{10}$$

in Equation 9 may be recognized as a constant, since both numerator and denominator are proportional to the square root of the radiated power when the antenna is transmitting. This factor will be called A. Therefore, Equation 9 may be rewritten as

$$v_L = \lambda 2\sqrt{2}\ A\, e(\theta, \phi)\, \frac{\sum_{n=0}^{N-1} \sqrt{G_n}\ \exp(j\, k\, n\, d \cos\theta)}{G_L + \sum_{n=0}^{N-1} G_n} \tag{11}$$

The effect of the on-off switches as described in the introductory statements is to make the various G_n step functions of time. This may be represented mathematically as

$$G_n(t) = G_n' \left[u\ (t - t_n) - u\ (t - t_n - \tau_n)\right] \tag{12}$$

where the G_n' are independent of time and where the τ_n are assumed to be much greater than the r-f period. Therefore, by controlling the various t_n and τ_n, the effective radiation pattern may be made to switch sequentially through a number of patterns. If the switching sequence is made periodic with period T it is possible to produce a pattern at one of the resulting spectral frequencies which has lower sidelobes than the unswitched, or static pattern. Specifically, examine the frequency component at the incident r-f frequency. This is given by

$$\langle v_L \rangle = \frac{1}{T} \int_0^T v_L\, dt = A2\sqrt{2}\, e(\theta, \phi) \frac{\lambda}{T} \int_0^T \frac{\sum_{n=0}^{N-1} \sqrt{G_n}\ \exp(jknd \cos\theta)\, dt}{G_L + \sum_{q=0}^{N-1} G_q} \tag{13}$$

From Equation 13 it is evident that for each value of n, the integral corresponds to an element excitation coefficient different from the static values for the array, i.e., the values when all elements are on. Therefore, by proper selection of switching times, it may be possible to improve the pattern sidelobe levels.

For example, assume that without switching the G_i' are chosen to give a particular aperture distribution. These then are not available for further adjustment. Assume also that N is odd and that the static aperture distribution is symmetrical about its center element. Then

$$G_i' = G_{N-1-i}' \qquad i = 0, 1, \ldots \frac{N-3}{2} \tag{14}$$

The new aperture distribution is specified to be symmetrical also and will be obtained by adjusting the on times of the elements in a symmetrical manner. The form of the switching is shown in Figure 3.

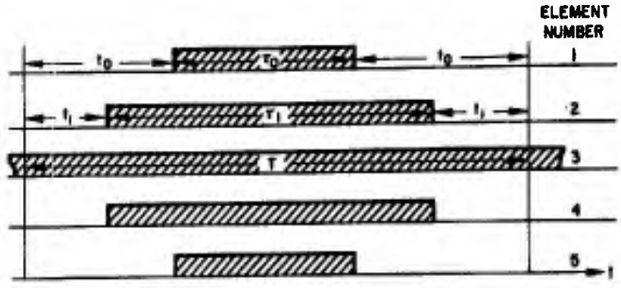

Figure 3. Illustrative excitation for five-element array.

This form of excitation is described by the following relationships.

$$\begin{aligned} t_i &= t_{N-i-1} \\ \tau_i &= \tau_{N-i-1} \\ \tau_i &< \tau_{i+1}, \qquad i < \frac{N-1}{2} \\ \tau_i &> \tau_{i+1}, \qquad i > \frac{N-1}{2} \\ T - \tau_i &= 2\, t_i \end{aligned} \tag{15}$$

If a new pattern of the form

$$h(\theta, \phi) = e(\theta, \phi) \sum_{n=0}^{N-1} a_n \exp(jknd\cos\theta) \tag{16}$$

is desired, then from Equation 11 the following relationships must be satisfied.

$$Ka_n = Ka_{N-1-n} = \sqrt{G'_n} \sum_{i=0}^{n} \frac{\tau_i - \tau_{i-1}}{T\left(G_L + \sum_{m=i}^{N-1-i} G'_m\right)} \qquad (17)$$

where

$$\tau_{-1} \equiv 0.$$

This provides an iterative procedure for determining the required on times of the elements. The constant K can be adjusted so that the center element is always on. A similar procedure holds true for an even number of elements.

A somewhat more easily realized switching scheme is illustrated in Figure 4. In this case all elements are switched on simultaneously and the control problems are reduced. Since the form of the distribution is obtained merely by bisecting that of Figure 3, the resulting expressions for determining the various τ_i are still given by Equation 17.

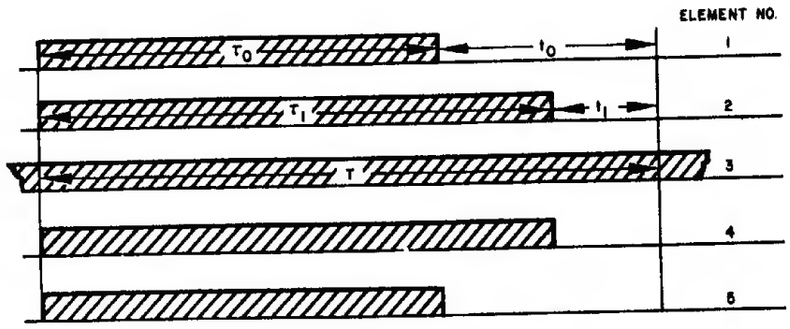

Figure 4.

Simplified Experimental Array

The foregoing illustrates the design of a low sidelobe time domain array in which the interactions of the array admittances are taken into account. However, to avoid the necessity of taking account of them in

an experimental array an antenna may be designed which contains isolators between the switches and the points where the branch guides couple to the main guide. Thus the input impedance of the array is essentially independent of the switching. The static aperture distribution may be obtained by use of attenuators and phase shifters in the branch lines and the switching will be used to improve the sidelobe level. For this case the received voltage is given by

$$v_L = \lambda \sqrt{\frac{2}{\pi}} \frac{\sqrt{G_{in}}}{G_L + G_{in}} \sqrt{\alpha \mathcal{G}_d(\theta, \phi)} \exp(j\zeta) \tag{18}$$

where G_{in} is the array input conductance and is now constant, α is the array efficiency factor that takes account of the presence of isolators and attenuators and $\mathcal{G}_d$ is the directive gain of the array. The factor α may be written as

$$\alpha = \frac{\sum_n G_{n_{ON}} \gamma_n}{G_{in}} \tag{19}$$

where $G_{n_{ON}}$ are the conductances which the branch lines present to the main line and the γ_n account for the attenuator settings in the branch lines. The summation is only over the elements which are ON. $\mathcal{G}_d$ is given by

$$\left[\mathcal{G}_d(\theta, \phi)\right]^{1/2} \exp(j\zeta) = \frac{2\sqrt{\pi}\, e(\theta, \phi) \sum_n \sqrt{G_{n_{ON}} \gamma_n} \exp(j\, k\, n\, d \cos\theta)}{\left(\sum_p \sum_q \sqrt{G_{p_{ON}} \gamma_p G_{q_{ON}} \gamma_q}\, I_{pq} \right)^{1/2}} \tag{20}$$

and the voltage becomes

$$v_L = \frac{2\sqrt{2}\lambda}{(G_L + G_{in})} e(\theta, \phi) \frac{\sqrt{\sum_i G_{i_{ON}} \gamma_i} \sum_n \sqrt{G_{n_{ON}} \gamma_n} \exp(j\, k\, n\, d \cos\theta)}{\left(\sum_p \sum_q \sqrt{G_{p_{ON}} \gamma_p G_{q_{ON}} \gamma_q}\, I_{pq} \right)^{1/2}} \tag{21}$$

Once again as in Equation 10 and the paragraph following it

$$\frac{\sqrt{\sum_i G_{i_{ON}} \gamma_i}}{\left(\sum_p \sum_q \sqrt{G_{p_{ON}} \gamma_p G_{q_{ON}} \gamma_q} \; I_{pq} \right)^{1/2}} = A_1 \qquad (22)$$

and there results

$$v_L = \frac{2\sqrt{2}\,\lambda}{G_L + G_{in}} A_1 \, e(\theta, \phi) \sum_n \sqrt{G_{n_{ON}} \gamma_n} \exp(j k n d \cos\theta) \qquad (23)$$

For the type of switching considered above this leads to the following relation between the coefficients of the time average pattern and the static pattern

$$Ka_n = Ka_{N-1-n} = \sqrt{G_n \gamma_n} \; \frac{\tau_n}{T} \qquad (24)$$

Thus an iterative procedure for determination of the τ_n is no longer necessary. The ratio of time average excitation coefficients to static coefficients is then directly proportional to the ratio τ_n/T.

Experimental Array

Based on the above discussion and design considerations, an array of eight collinear slots with on-off switching control is under construction to demonstrate experimentally the sidelobe reduction technique. A diagram of this array and its subsequent microwave network is shown in Figure 5. Certain of its features are summarized below:

a. The position of each slot relative to its waveguide was designed to be identical; consequently, all the slots are of equal conductance. The relative excitation amplitude of the slots is controlled by

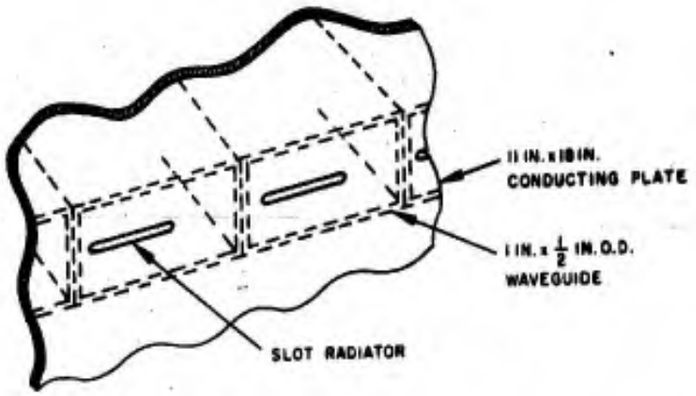
11 IN. x 18 IN.
CONDUCTING PLATE
1 IN. x 1/2 IN. O.D.
WAVEGUIDE
SLOT RADIATOR

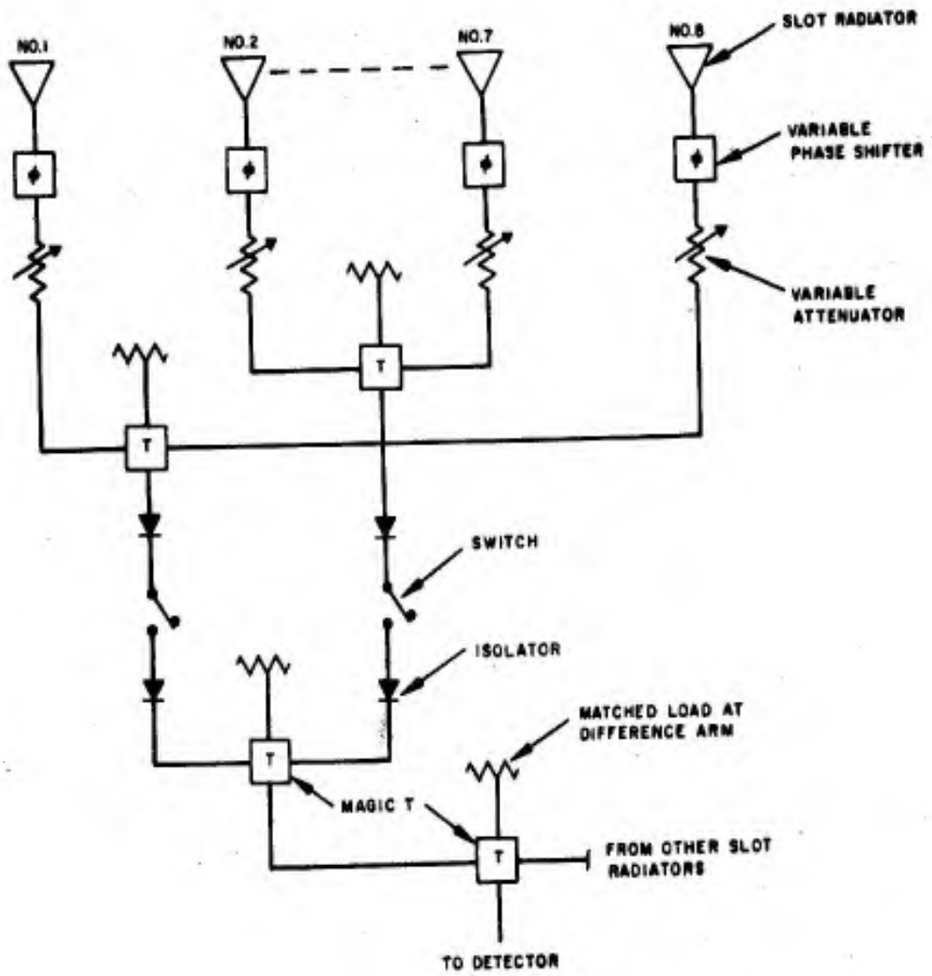
NO.1
NO.2
NO.7
NO.8
SLOT RADIATOR
VARIABLE
PHASE SHIFTER
VARIABLE
ATTENUATOR
T
SWITCH
ISOLATOR
MATCHED LOAD AT
DIFFERENCE ARM
MAGIC T
FROM OTHER SLOT
RADIATORS
TO DETECTOR

Figure 5.

the attenuators instead of by displacements of the slots off the centerline of the waveguide. The desired static distribution may be obtained by proper adjustments of the attenuators.

b. The relative phase of each element is controlled by a calibrated precision phase shifter; thus the problem of the tolerance in slot length is removed.

c. The slots are collinear. This eliminates second-order beams in directions not exactly normal to the ground plane in which the slots are cut. (See section on Second Order Beams in this report.)

d. The mutual coupling effects between slots are reduced since the element factor of a slot is minimum in the direction of its neighbors.

e. The efficiency of the array is reduced to a certain extent due to the fact that some energy is absorbed by the attenuators in the lines. However, for demonstration purposes this is not considered of great importance.

The static aperture distribution has been chosen to be a 30-db Tschebyscheff for this experiment. The switching times have been selected to give a reduction in sidelobe levels to 40 db for the filtered component at the carrier frequency. The static excitation coefficients, the time average excitation coefficients and the required normalized on times τ_n/T are given in Table I.

Element Number	Static Coefficients		Time Average Coefficients		τ_n/T
	Ampl.	db	Ampl.	db	
1, 8	0.2621	-11.63	0.1460	-16.71	0.5571
2, 7	0.5185	-5.70	0.4178	-7.58	0.8056
3, 6	0.8118	-1.81	0.7593	-2.39	0.9354
4, 5	1.0000	0.000	1.0000	0.00	1.000

Table I. Experimental array design data.

When all the r-f circuitry and switch control circuitry is completed the desired aperture distributions will be set up and pattern measurements undertaken.

Sideband Frequency Characteristics

The use of periodic switching of the array elements introduces frequencies into the received signal other than the desired one, i.e., the carrier frequency. An analysis of the effective spatial patterns at the frequencies with the most significant amplitudes has been carried out. These are compared with the desired time average pattern in Figure 6. It is readily seen that the patterns corresponding to the first upper and lower sidebands are each approximately 21 db below the desired "time average pattern." Succeeding sideband patterns are even less significant. Thus relatively little power has been converted into unwanted sidebands. Neglecting higher frequency terms this represents a loss in available power of about 0.1 db as compared with an unswitched array with a 40-db Tschebyscheff pattern. If all the sidebands were taken into account the loss would be increased somewhat but not a significant amount. For example, if there were ten additional sidebands with the same level as the lowest considered in Figure 6, the loss would become 0.27 db. However, it is felt that this represents a very pessimistic condition and not a typical loss.

TRANSMITTER AND RECEIVER

In the experimental program a CW transmitter is used. The output of the receiving antenna consists of a carrier and sidebands separated by multiples of the modulating frequency. It is seen then that the usual detection by the use of bolometers or crystals will not work since these devices measure the total power output without regard to frequency. Thus the detectors must include one or a set of narrow band filters. The receiver used here is a quadruple detection set using the superheterodyne principle.

As mentioned in the introduction, the signals between the transmitter and receiver must be coherent over the time required to process the signal. In the experimental program for this project a 10-kc

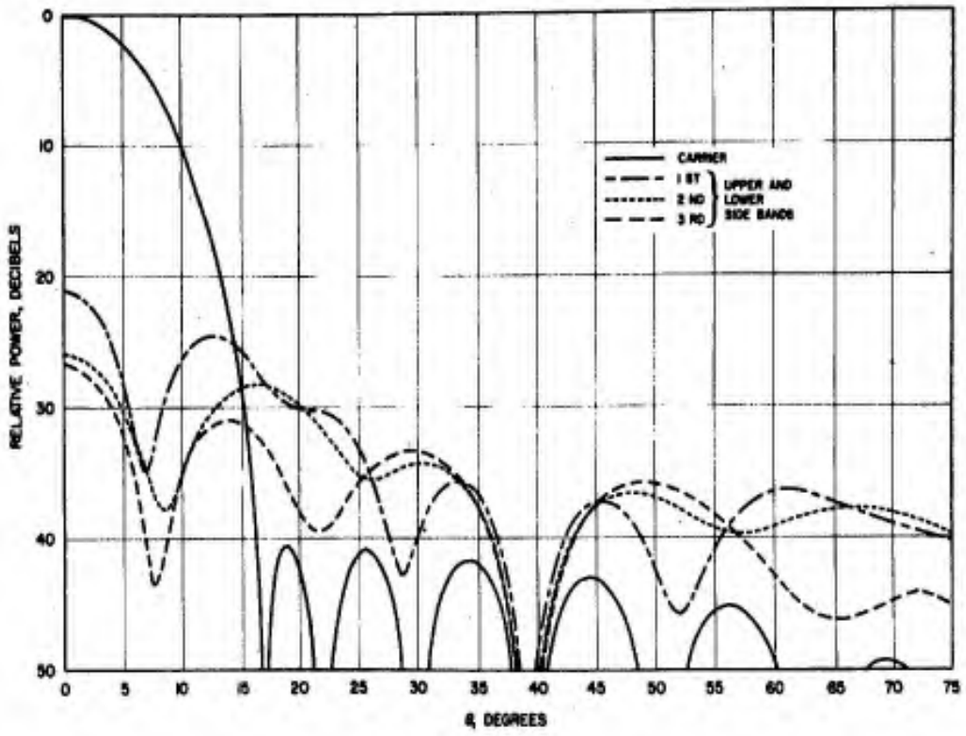

Figure 6. Calculated patterns of various frequency components of switched eight-element array.

modulating frequency was selected which means then that the array is switched in one tenth of a millisecond. Thus the coherence time should be of this order of magnitude.

The type of modulating devices determine the selection of the modulating frequency. In an earlier program in the time domain techniques (RADC Contract AF 30(602)-2021) ferrite devices were used as switches. These have inherently long time constants, thus requiring low-modulating frequencies. In this program the solid state diode switches used do not have this limitation. To make the system compatible with either type of switch the 10 kc modulating frequency was chosen as a compromise.

The low modulation frequency requires high transmitter and local oscillator stability, but simplifies the design of the timing circuits and of the driving circuits for the solid state switches. If the transmitter and local oscillator frequencies are derived from different sources it is convenient to have long-term coherence between them also. Since the sidebands at the output of the receiving antenna are 10 kc apart, a drift of the local oscillator beyond one sideband will require retuning to detect the correct sideband.

The requirements for the transmitter and receiver are as follows:

Transmitter frequency	9.375 kmc
Transmitter stability	Short term about 1 part in 10^{13} (1 ms)
	Long term, 1 part in 10^{8} (1 hour)
Receiver stability	Same as transmitter
Bandwidth	$<$10 kc
Dynamic range	$>$40 db

One relatively straight forward way to obtain a stable frequency is to use a stable crystal oscillator and multiply the output frequency the proper number of times to obtain the required X-band frequency. This method was employed in the present system. The crystal oscillator used consists of a crystal and transistor oscillator in a temperature-controlled oven.

Transmitter

A schematic diagram of the transmitter is shown in Figure 7.

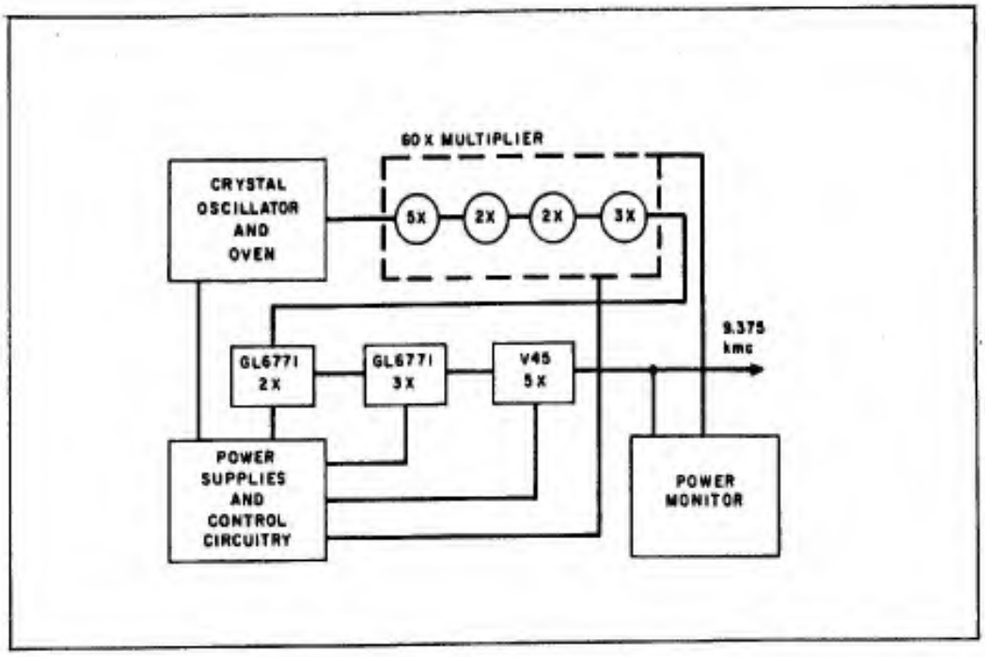

Figure 7.

The output of the crystal oscillator is 5v min across 5 kΩ at 5.20833 mc. The output of the 60 x multiplier is 25.8 dbm at 312.5 mc. The succeeding doubler has an output of 27.6 dbm at 625 mc. The input at 1875 mc to the V45 klystron is 22.9 dbm from the tripler.

At 9,375 mc about 13.8 dbm are realized. It is possible to get an output of 30 dbm at X-band with more drive on the V45.

A photograph of the transmitter is shown in Figure 8.

Receiver

In the sidelobe suppression experiments only the carrier contains useful information. The bandwidth of the receiver must be less than 10 kc so that the carrier may be separated from the sidebands. Since 40-db sidelobes are to be measured a dynamic range of 40 db or better

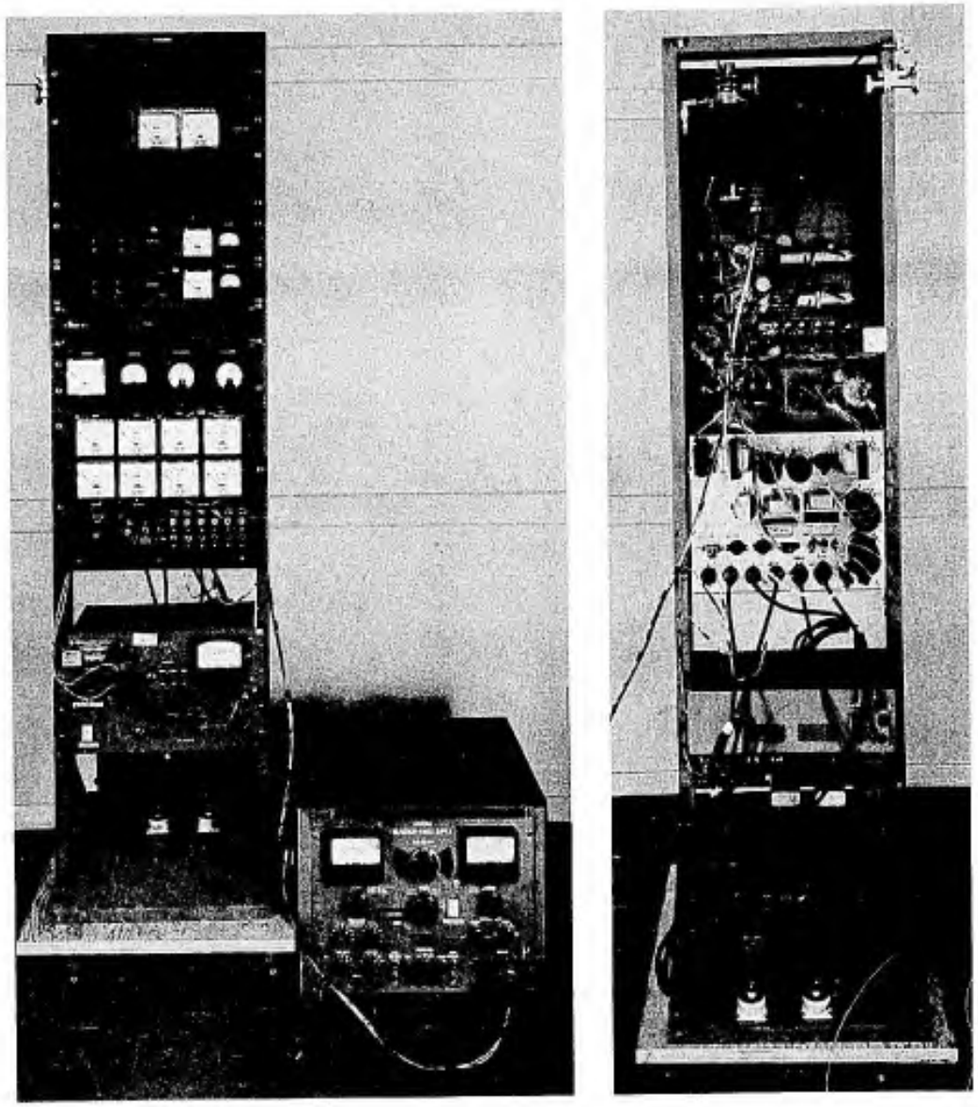

a. Front view. b. Rear view.

Figure 8. Transmitter.

must be incorporated into the receiver. A HAC designed receiver which meets these requirements is described below. It consists of a quadruple detection receiver whose bandwidth is 6 kc. It will be described with the aid of Figure 9.

The rf signal out of the receiving antenna is fed into a balanced mixer. The local oscillator is at 9.345 kmc. It is identical in design to the transmitter just described except that the crystal frequency is 5.191667 mc.

The output is at a frequency of 30 mc. The 30-mc signal and the sidebands are amplified in a 30-mc radar amplifier which incorporates an AGC circuit which is controlled by the dc from the last detector. The signal is then mixed with a crystal-controlled local oscillator. The output of the mixer is amplified in a 3-mc i-f strip with a bandwidth of 150 kc. The signal is mixed with the signal from a local oscillator with an adjustable frequency (2.75 mc $\pm$ 50 kc). The output of the mixer is amplified by a 250-kc i-f with a bandwidth of 6 kc. The bandwidth is obtained by a Collins mechanical filter whose bandwidth at the 60 db points is 14 kc. With the local oscillator set at 2.75 mc, the carrier frequency is detected. Any sideband may be detected by changing this local oscillator in 10-kc steps (i.e., for first upper sideband set local oscillator at 2.74 mc). High level a-c amplification is used after the amplifier. This is detected and part of the dc is fed back to the first i-f amplifier for AGC. Since no d-c amplification is used in the receiver a high degree of stability is realized. The receiver is stable to $\pm$1 db for 24 hours or longer.

A dynamic range of 30, 40, 50, or 60 db is obtained by a selector switch on the front panel. The output is -30 volts dc for a signal of -60 dbm input at 30 mc with 60 db compression. The minimum signal detectable is -130 dbm. Further mixing is done to reduce 250 kc to 5 kc for monitoring purposes. A frequency meter with 10 kc full-scale monitors the output frequency.

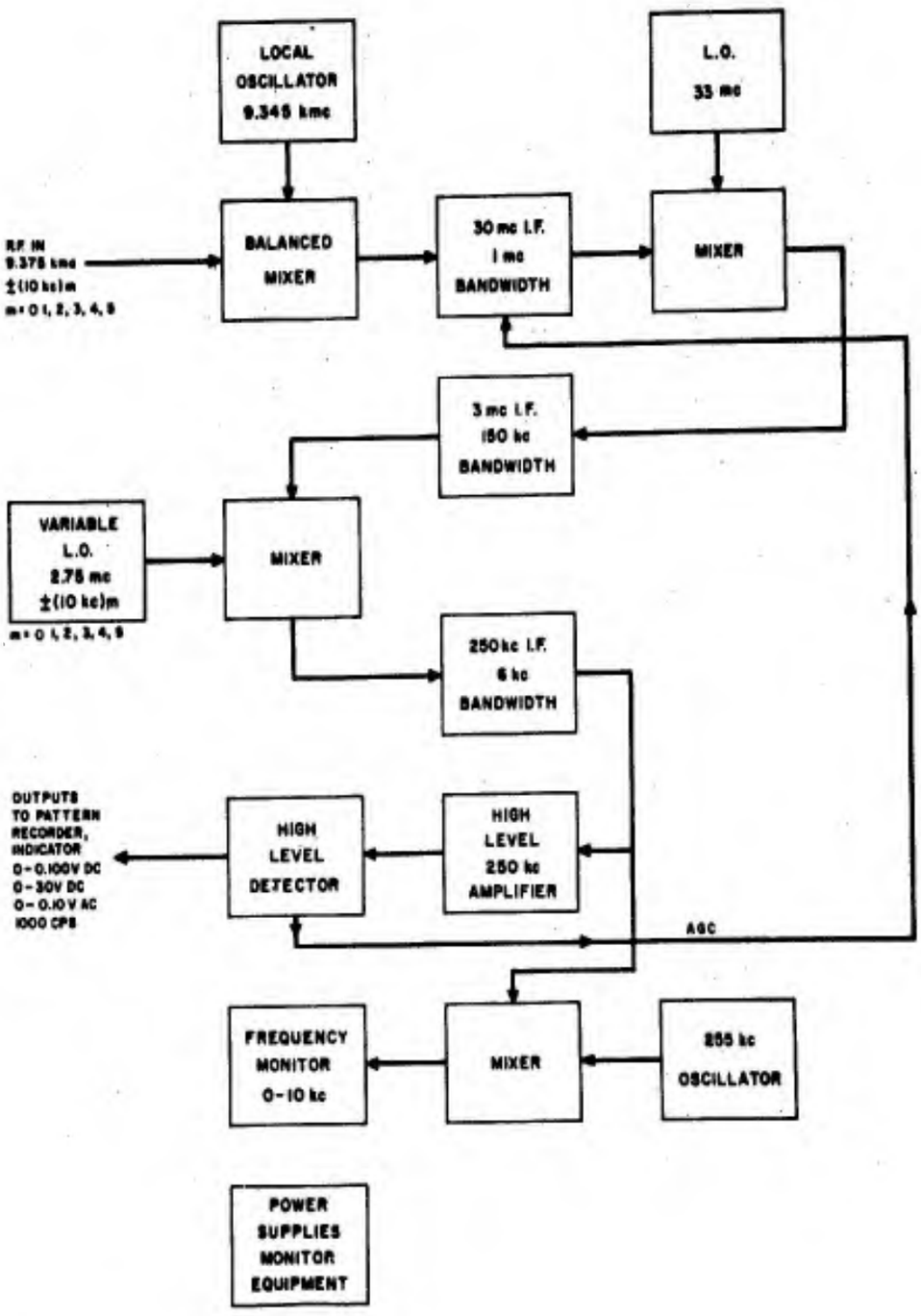

Figure 9. Block diagram of receiver.

The outputs available are

1. 0-30v dc
2. Meter 0-100
3. 0-0.100v dc
4. 0-0.100v ac 1000 cps.

The last is obtained by using the output of the 250 kc amplifier as a carrier in an AM modulator whose modulating frequency is a 1000-cps tuning fork oscillator. The modulating frequency is recovered by the usual detecting methods.

Tests show that the crystal oscillators have a stability better than that which can be determined by a Hewlett-Packard counter, Model 524D (which is ±1 part in 10^8). The total system stability as determined by our frequency meter on an expanded 0-1 kc full scale is better than ±33 parts in 10^9 in 8 hours. A sample recording is shown in Figure 10.

RF SWITCHES AND PROGRAMMING CIRCUITS

The applications of time domain techniques being considered in this study employ on-off switching of the elements in microwave antenna arrays. The switching techniques require fast acting electronically controlled rf switches with good switching ratios, and control circuitry to actuate the switches. This section discusses the rf switches and describes the associated control circuitry that has been developed.

RF Switches

The rf switches required for time domain applications must be fast acting, provide high switching ratios and need handle only low rf power. Semiconductor diode switches provide these characteristics. Accordingly a switch was developed which employs two 1N263 germanium diodes, each mounted directly across a section of X-band waveguide, and separated along the guide axis by three fourths of a guide wavelength. The diodes are mounted in holders designed by Hughes Aircraft Company. The switch parameters are somewhat sensitive to diode positioning but once adjusted and locked in place they operate satisfactorily. The following are typical properties of the switches.

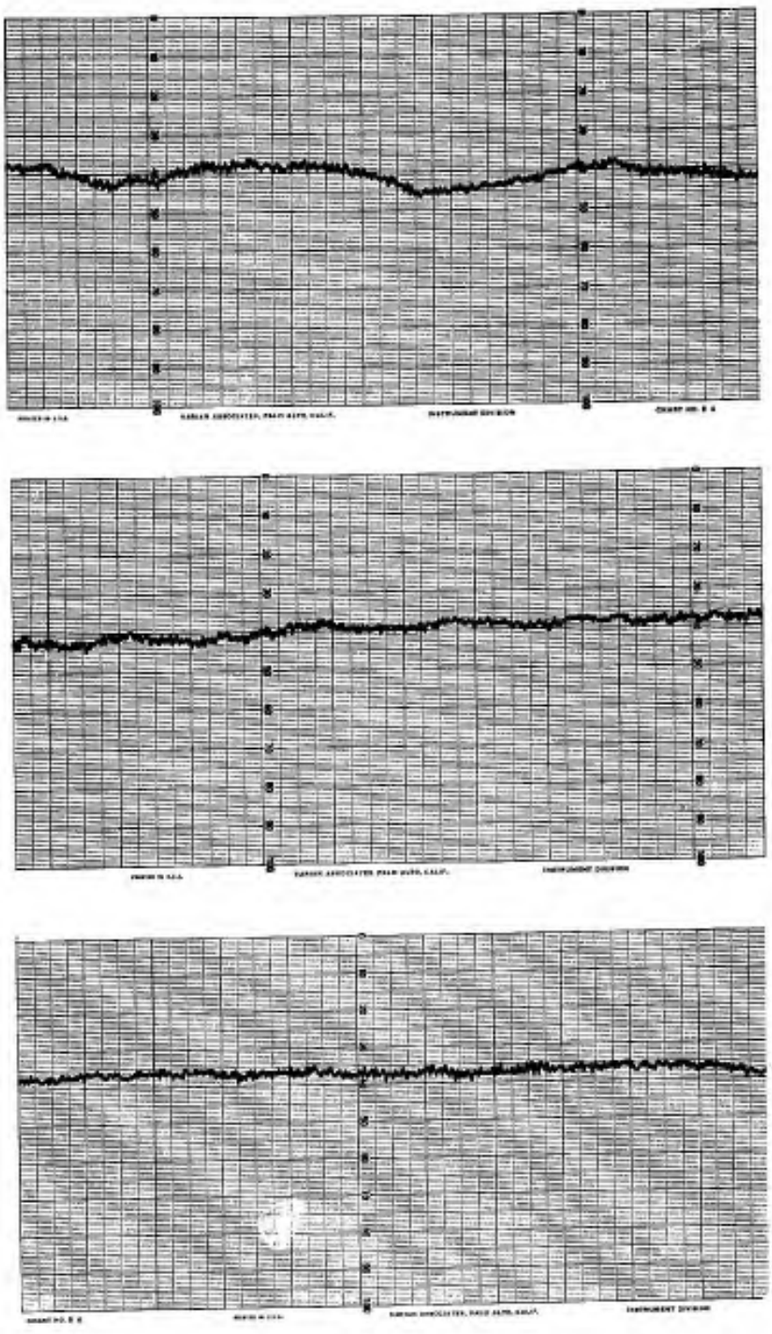

Figure 10. System frequency stability, 10 cps/div - chart speed 6 inches per hour.

Input VSWR–on	1.1 to 1.2
Input VSWR–off	25
Insertion loss–on	2.5 to 3 db
Switching ratio	45 to 55 db
Control voltage–on	0.7 to 0.8 volts dc
Control current–on	60 to 80 ma. dc
Control voltage–off	-0.7 to -0.8 volts dc

The switching times of the switches themselves have not been measured, but based on available literature they are expected to be of the order of a few nanoseconds. In application, switching times will be determined by the external control circuitry as mentioned below. Figure 11 shows the assembled switch.

Programming Circuits

For the sidelobe suppression application the rf switches must be switched on simultaneously and then be individually turned off at times τ_m later. This has been discussed earlier in the report. This switching is done periodically with period T which has been selected as 10^{-4} seconds. Therefore proper switching requires generation of positive current pulses with widths variable over the range of τ_m required. For the array described the τ_m/T range from about 0.50 to 0.95. Three switches with individually controlled pulse widths are required for the experimental array. The required control circuitry has been developed and a block diagram is shown in Figure 12. The repetition rate is furnished by a 10 kc crystal controlled oscillator, which drives a pulse generator producing 10-kc negative spikes. Beyond this stage three parallel channels are used, one for each switch. In each channel the 10-kc negative timing spikes enter a pulse width control where the spikes become flat pulses having duty cycles adjustable from 0.03 to 0.98. Each generator has a memory flip-flop which turns on with the application of an input spike and turns off when the delayed pulse leaves. The variable width output pulse is taken from this memory circuit through an added buffer circuit. The negative rectangular pulses are fed through

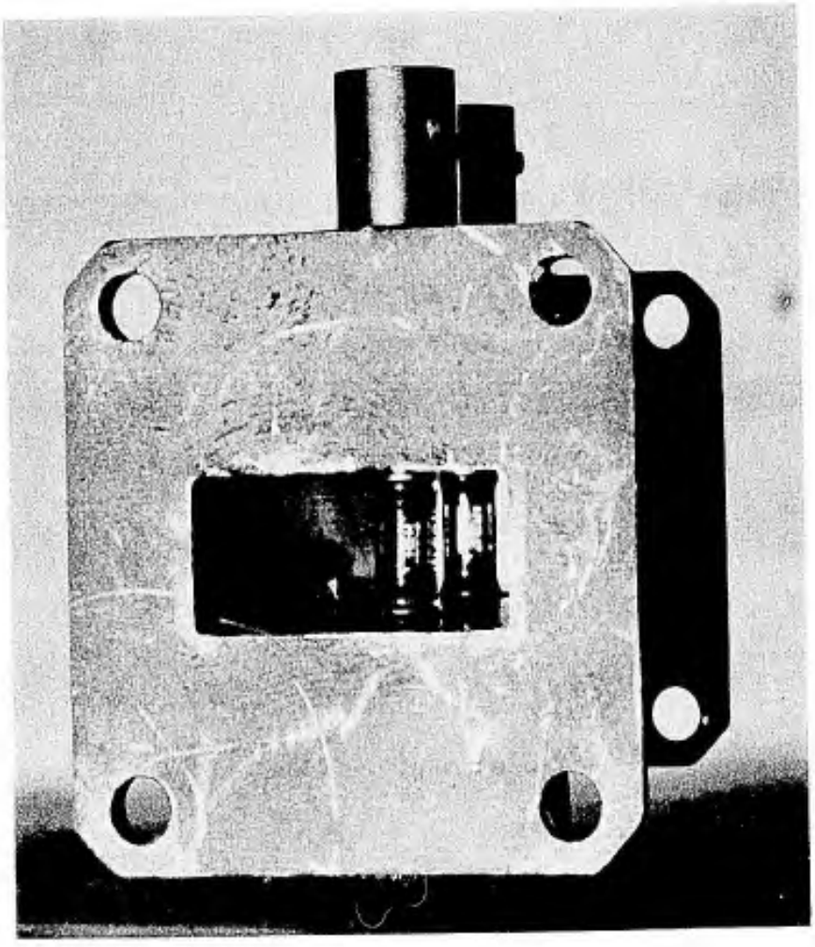

Figure 11. Assembled waveguide switch showing positions of diodes.

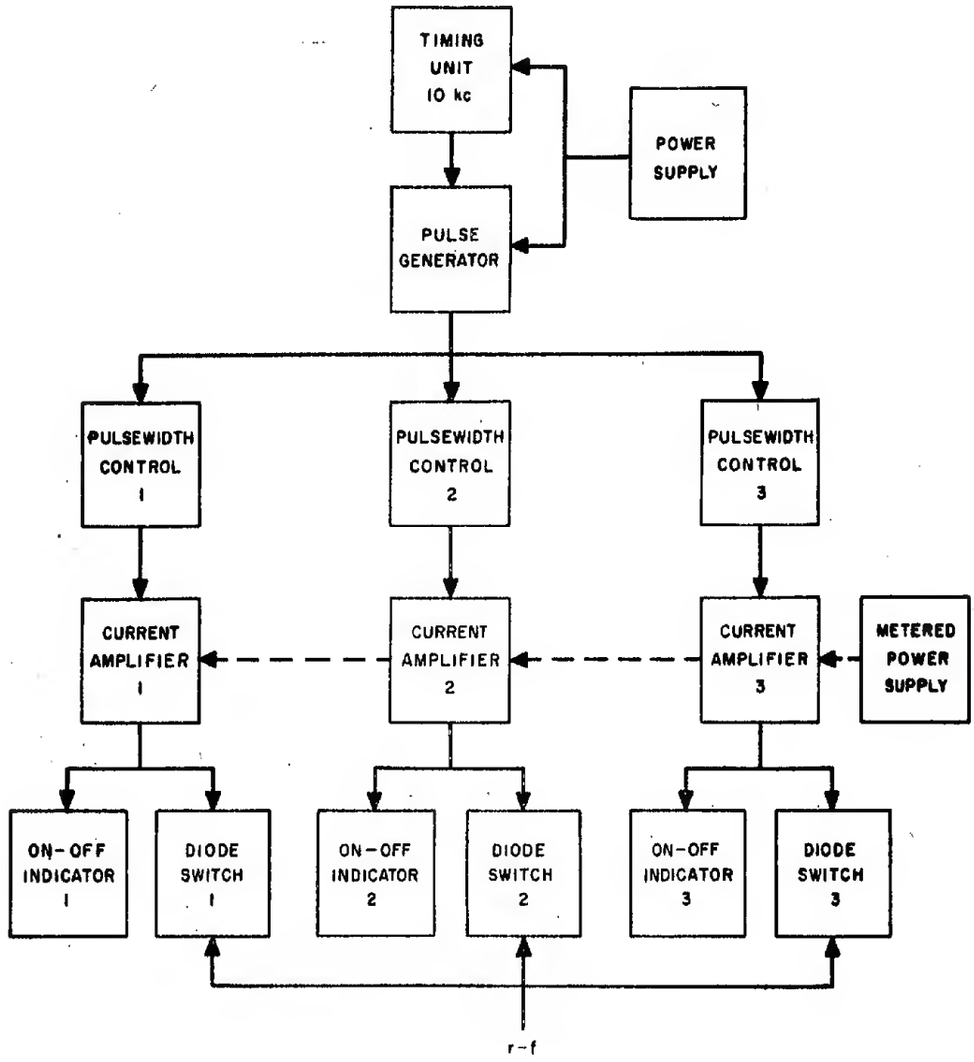

Figure 12. Block diagram of switching circuitry.

an inverting current amplifier to both the diode switches and on-off indicators. Neon bulbs are used as indicators; one firing with the switch on, the other firing with the switch off. Power supplies for the current amplifiers consist of a metered box of batteries. Each switch can be turned on or off or programmed.

The resultant microwave energy transmitted through the switch consists of rectangular pulses adjustable from 3 to 98 μsec duration and having a 100 μsec repetition period. Rise and fall times of 0.1 μsec are expected with the final configurations. Figure 13 shows the current amplifier driver with cover plate removed. Figure 14 shows the amplifier mounted directly on the rf switch.

PATTERN RANGE TESTING

The ground reflection measurements of the antenna range have been completed. The reflected signals from the ground were more than 60 db below the direct path radiation with an exception of two spots which were down about 56 db. They can probably be corrected by moving some earth near these areas to redirect the scattered signal. The measurement procedure has been described in detail in the previous report. (RADC-TN-61-145.)

Earlier measurements have shown that the reflected signal from the receiving antenna mount and its vicinity was quite significant, consequently a flat surface 9 feet × 5 feet covered with Eccosorb CV6 was used in order to eliminate the unwanted reflection. A sketch illustrating the arrangement is shown in Figure 15. Further investigation of the range characteristics has been continued with a linear standing wave slot array as the receiving antenna.[5] This array has 32 elements, and was designed to have a sidelobe level of 30 db with a Taylor distribution.[6] The design pattern, the pattern calculated from the measured displacements of the slots, and the measured patterns, are shown in Figures 16 and 17. Since the sidelobes of this array are low, the change in sidelobe structure due to reflected signals can be detected quite easily. Furthermore, the element factor of the slots in the array is nearly a

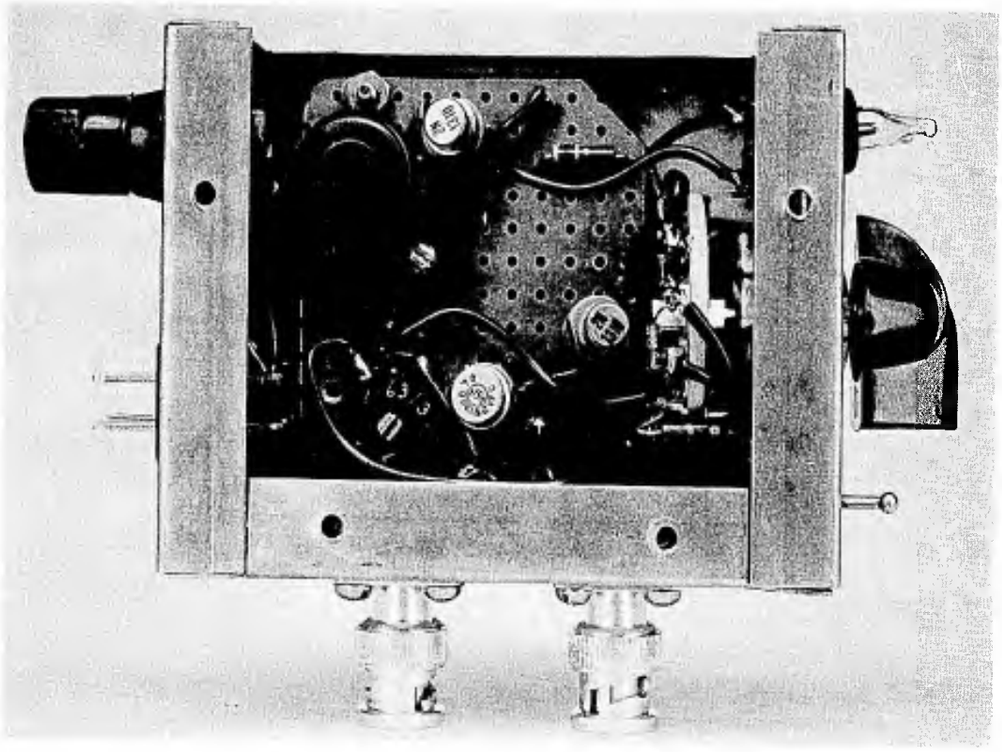

Figure 13. Current amplifier for waveguide switch with cover plate removed.

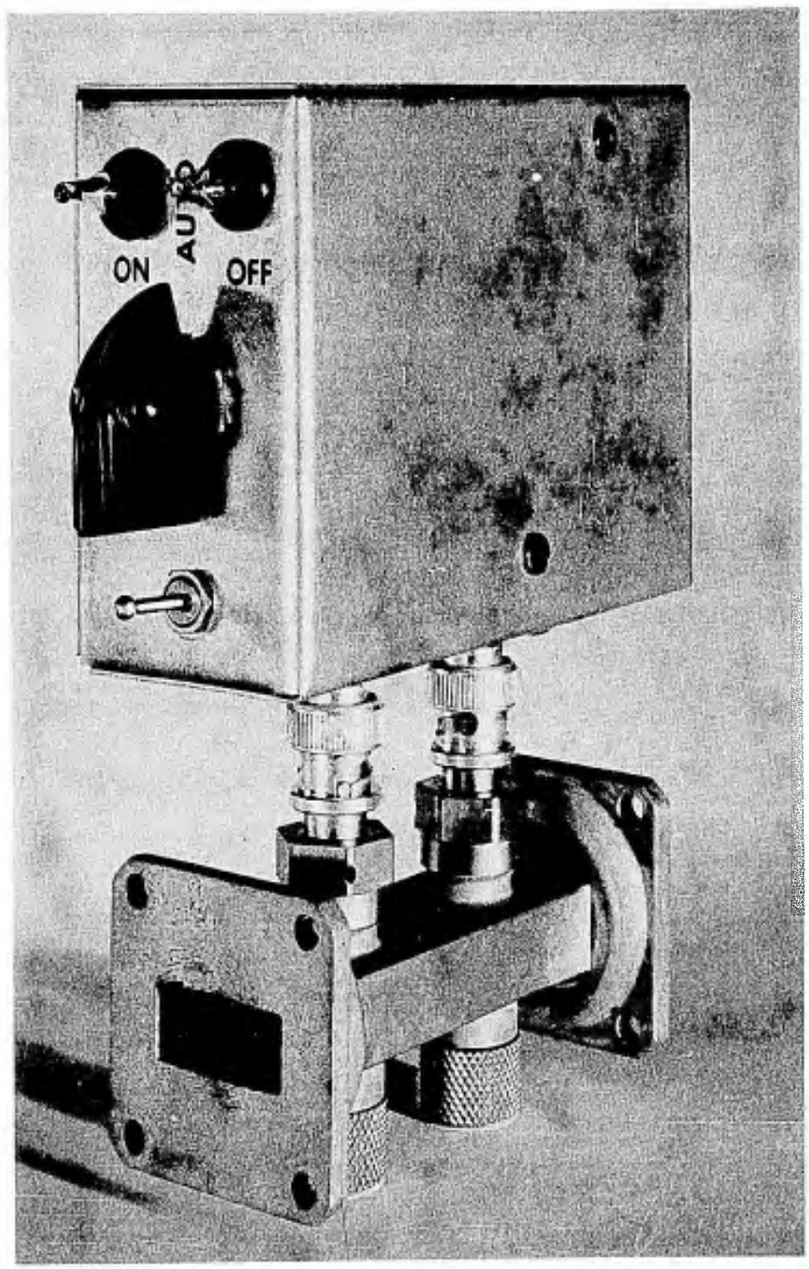

Figure 14. Completed waveguide switch and current amplifier assembly.

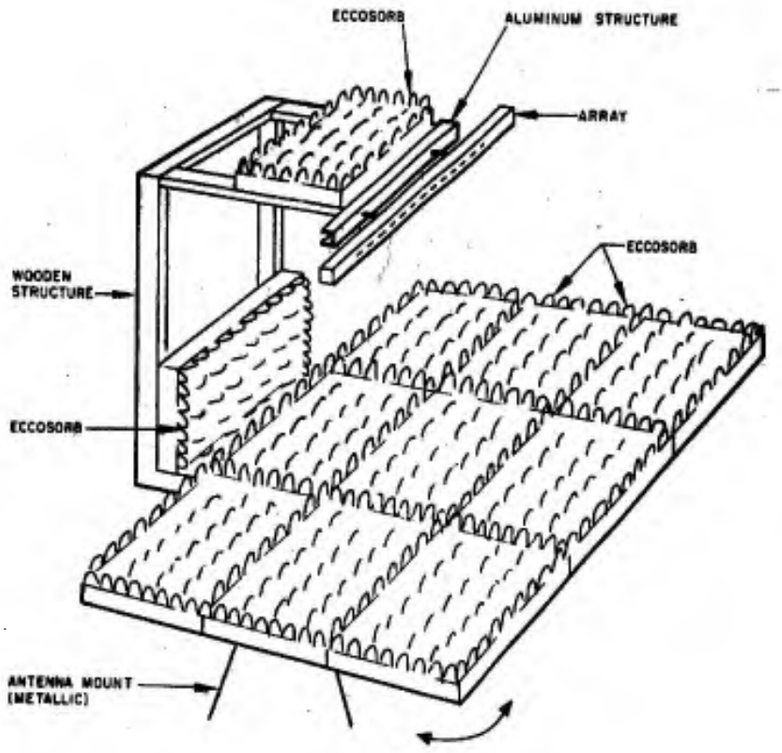

Figure 15. Sketch of platform and array support showing Eccorb covering.

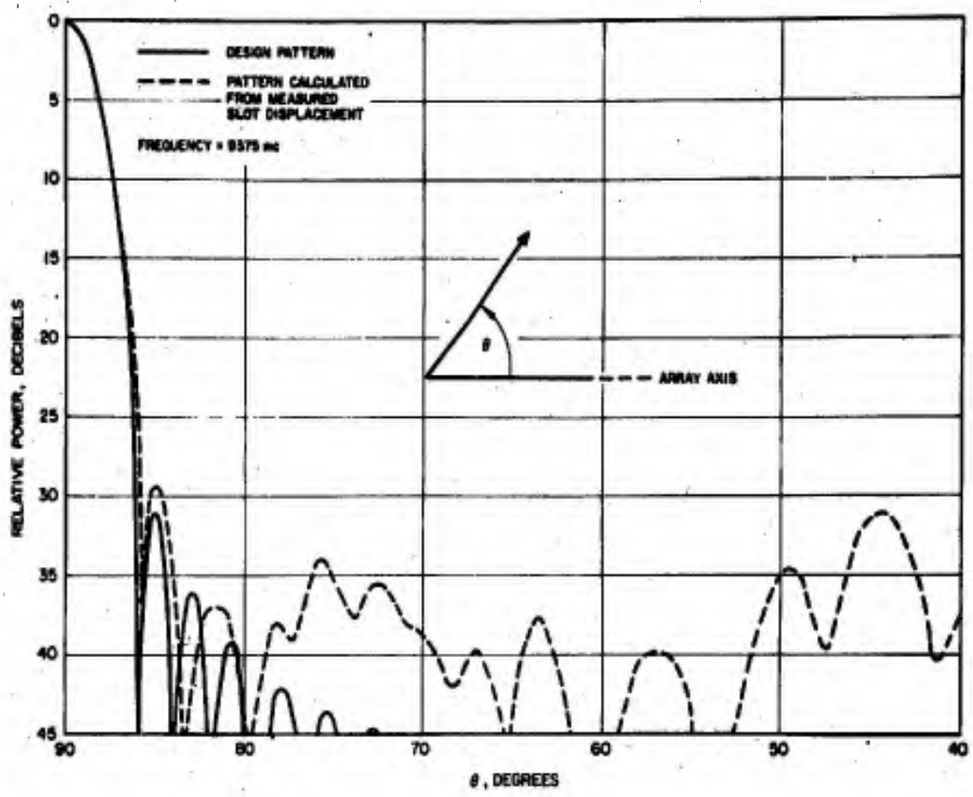

Figure 16. Patterns of 32 element array used in pattern range tests.

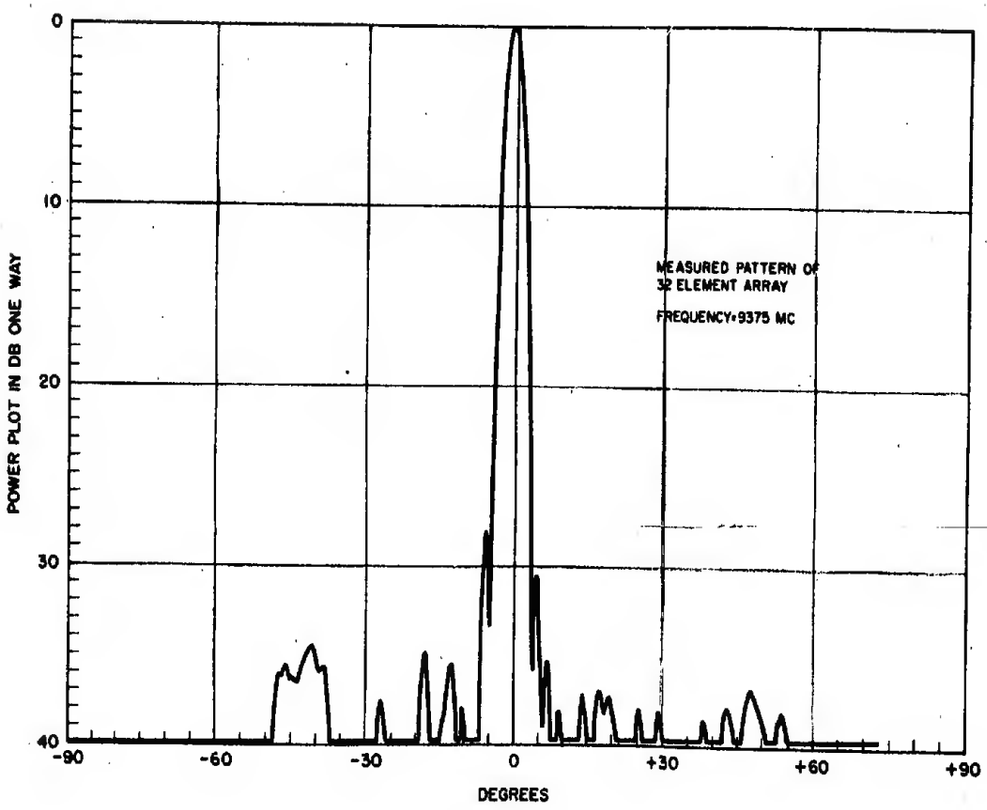
0
10
20
30
40
POWER PLOT IN DB ONE WAY
MEASURED PATTERN OF
32 ELEMENT ARRAY
FREQUENCY-9375 MC
-90
-60
-30
0
+30
+60
+90
DEGREES

Figure 17.

constant in the plane perpendicular to the array, hence, in comparison with parabolic reflector antennas, it is very sensitive to reflected signals in this plane.

Patterns were taken with the array at various positions displaced along its axis as shown in Figure 18. Care was taken to keep the array level and normal to the direction of the incident signal. Displacements of d = 0.32λ, 0.56λ, and 0.71λ were tested. By displacing the array a distance

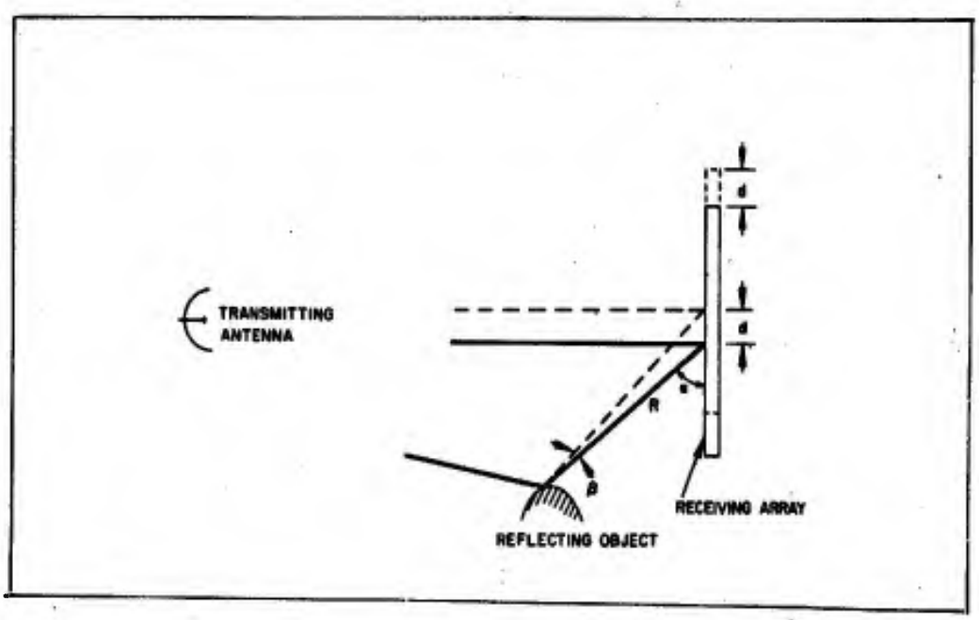

Figure 18.

d, the reflected signal arriving at the receiving antenna would be different in phase by $\frac{2\pi}{\lambda}\left(R - \sqrt{R^2 + d^2 + 2Rd\cos\alpha}\right)$. Suppose the distance of the reflecting object to the array is sufficiently large in comparison with d so that β is small, say $\beta < 5^{\circ}$. This assumption is legitimate since there is no reflecting surface close to the array. For $R \gg d$, the above phase difference expression would be reduced to approximately

$\frac{2\pi}{\lambda} d \cos \alpha$. A significant phase change would be obtained for the above d values provided α is not close to 90°. If there were any sufficiently high reflected signals (not from α close to 90°), the change in sidelobe structure would be detected. For those four array positions, the patterns were fairly repeatable, no change greater than 1 db was noticed in any sidelobe. The patterns are shown in Figures 17, 19, 20 and 21.

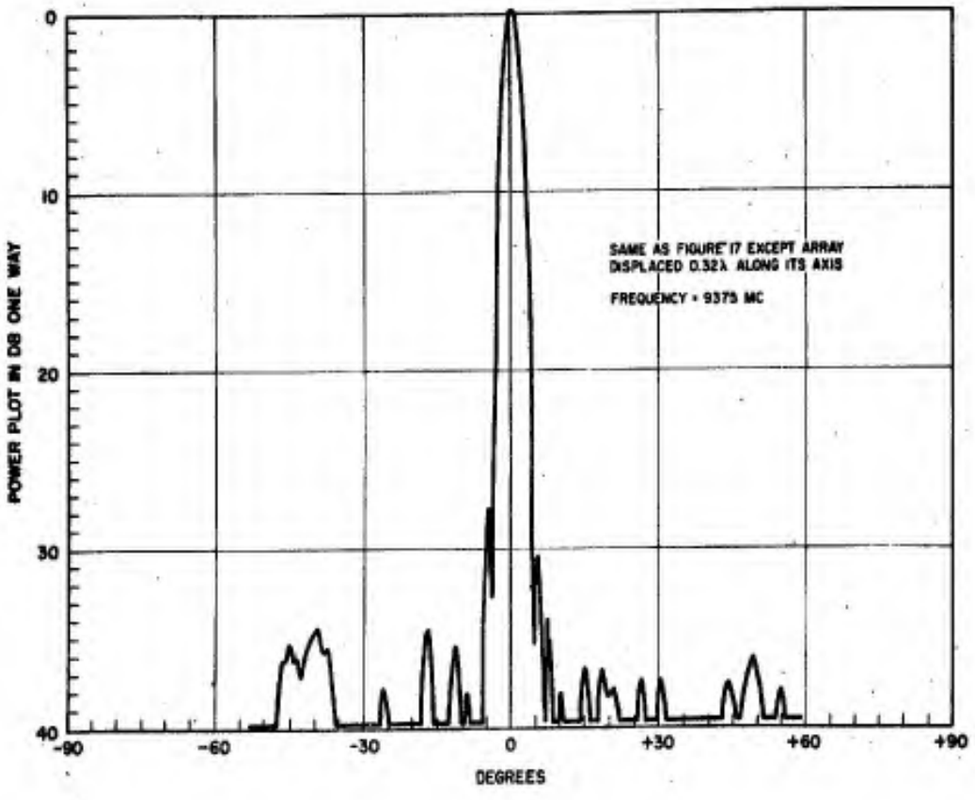

Figure 19.

As a further check, another method for testing the reflected signals was made by reversing the array end for end. If there are no extraneous reflections, the patterns should be the images of each other about broadside. Many patterns were taken, and no significant changes were noticed except for the lobes at approximately ±45°. A typical pair

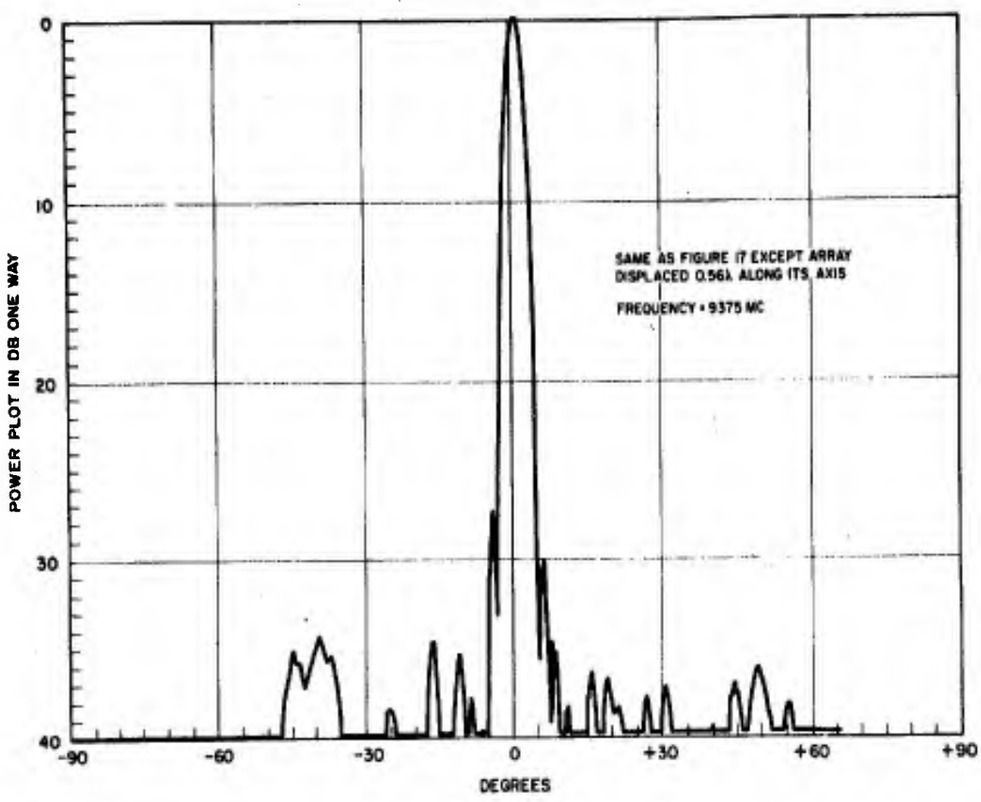

Figure 20.

of patterns is shown in Figures 17 and 22. The $\pm 45^{o}$ lobes are a consequence of the fact that the slots in the test array are not collinear and the pattern was taken in the plane not exactly containing the array and the transmitting antenna. Any slight change in array position which causes the array to be not exactly normal to the incident signal would alter the lobes at $\pm 45^{o}$ considerably. During the reversing process, some small error in positioning the array can easily occur. Though, for the dimension parallel to the array axis, the array can be made horizontal easily by use of a level, the other dimension of the array is only one-half inch, hence it is extremely difficult to place the array normal to the transmitter to the desired accuracy. An analysis of these lobes is given in the following paragraph. From the above results in

measurements, it may be concluded that a 40 db sidelobe array can be measured to an accuracy of ±1.5 db.

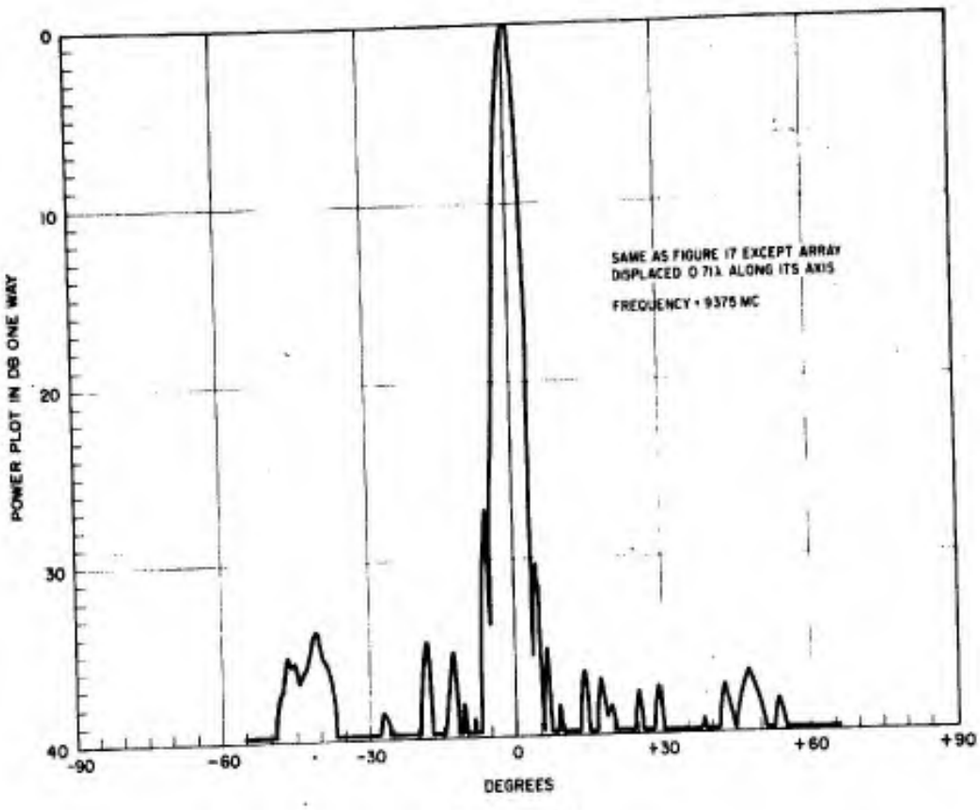

Figure 21.

Second-Order Beam

The second-order beam referred to above is caused by the non-collinear nature of the slots in the array.[7] The dependence of the second-order beam on the array positioning may be seen from the following.*

*A different analysis concerning this subject may also be seen in reference 7 in which the array is assumed to consist of two parallel linear arrays separated by twice the "weighted" mean slot offset. The direction (for both θ and ϕ) of the peak of the second-order beam is analyzed there.

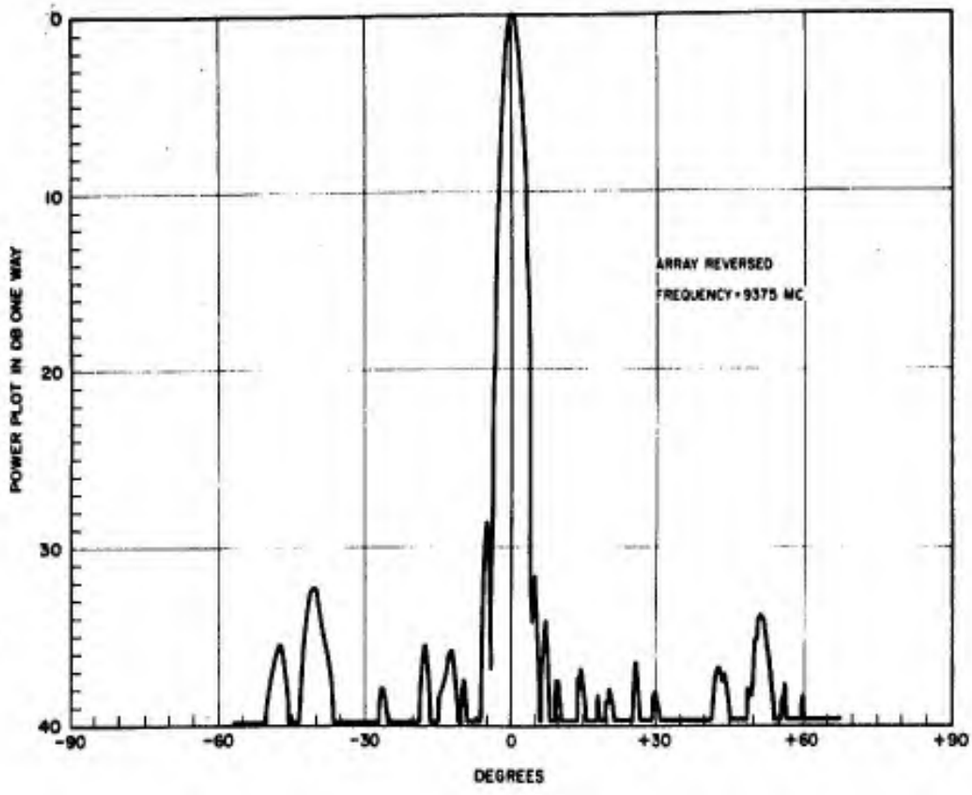

Figure 22.

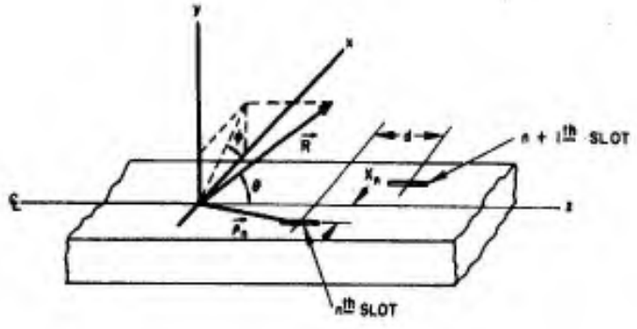

Figure 23.

For our purpose here, we are concerned only with ϕ close to 90°, and the objective is to find the change in the radiation pattern as a function of θ caused by the second-order beam for some small range of ϕ.

Assume that the aperture distribution is symmetrical and the array consists of an even number of slots (the latter assumption is not essential). The field intensity is given by[3]

$$E(\theta, \phi) = e(\theta, \phi) \sum_n A_n \exp(jk \vec{R} \cdot \vec{\rho}_n) \tag{25}$$

where $e(\theta, \phi)$ is the element factor, $\vec{R}$ is a unit vector in the direction (θ, ϕ), A_n are the excitation coefficients of the array and $\vec{\rho}_n$ is the displacement vector of the nth slot. For a standing wave broadwall shunt slot array, the elements are one-half guide wavelength apart and the consecutive elements are located on the opposite side of the z-axis. Thus

$$\vec{R} \cdot \vec{\rho}_n = nd\cos\theta + x_n \sin\theta \cos\phi,$$

and

$$\begin{aligned} E(\theta, \phi) &= e(\theta, \phi) \sum_n A_n \exp(jknd\cos\theta) \exp(jkx_n \sin\theta \cos\phi) \\ &= e(\theta, \phi) \sum_n A_n \exp(jknd\cos\theta) \left[1 + jkx_n \sin\theta \cos\phi \right. \\ &\qquad \left. - \frac{1}{2}(kx_n \sin\theta \cos\phi)^2 + \ldots\right] \end{aligned} \tag{26}$$

Suppose an error in positioning the array is less than 5°, that is $|90^{\circ} - \phi| < 5^{\circ}$. In other words, the radiation pattern is taken in a plane not more than 5° off the plane containing the transmitting antenna and the array axis. For an ordinary array,[6] $|x_n| \leq 0.08''$, then

$$\begin{aligned} \frac{1}{2}\left|kx_n \sin\theta \cos\phi\right|^2_{\text{max.}} &= \frac{1}{2}\left|\frac{2\pi}{1.26''}(.08'') \sin 90^{\circ} \cos(90^{\circ} \pm 5^{\circ})\right|^2 \\ &< 6.2 \times 10^{-4} \text{ radians} \end{aligned} \tag{27}$$

and Equation 26 may be written as

$$E(\theta,\emptyset) \approx e(\theta,\emptyset) \sum_n A_n \exp(jknd\cos\theta) + jk\sin\theta\cos\emptyset\, e(\theta,\emptyset) \sum_n A_n x_n \exp(jknd\cos\theta) \tag{28}$$

The field intensity $E(\theta,\emptyset)$ may be treated as the sum of two terms, a term $e(\theta,\emptyset) \sum_n A_n \exp(jknd\cos\theta)$ which represents the ideal field and a term $jk\sin\theta\cos\emptyset\, e(\theta,\emptyset) \sum_n A_n x_n \exp(jknd\cos\theta)$ which may be thought of as the error term.

The maximum contribution of the error term to the field pattern as a function of θ may be calculated exactly if desired, but the computation would be quite involved. However, with the knowledge of the behavior of the factor $e(\theta,\emptyset)\sin\theta$, it may be concluded safely that the maximum of the error term occurs in the immediate neighborhood of the maximum of the factor $\sum_n A_n x_n \exp(jknd\cos\theta)$. Since x_n and x_{n+1} are opposite in signs, the absolute maximum of $\sum_n A_n x_n \exp(jknd\cos\theta)$ occurs when

$$kd\cos\theta = p\pi, \quad p = \text{odd integers.} \tag{29}$$

For nonmultiple beam arrays, (i.e., $d<\lambda$), $|p|\leq|$. Now, take the value of θ which satisfies Equation 29 and denote it by θ_m.
Then

$$\left|\sum_n A_n x_n \exp(jknd\cos\theta_m)\right| = \sum_n \left|A_n x_n\right| . \tag{30}$$

For low sidelobe arrays in general, and for $\left|90^\circ - \emptyset\right|$ near 5° such that $k\sin\theta_m\cos\emptyset\, e(\theta_m\emptyset) \sum_n \left|A_n x_n\right|$ is sufficiently greater than $\left|\sum_n A_n \exp(jknd\cos\theta)\right|$ for θ in the neighborhood of θ_m, the direction of the second-order beam is approximately at the angle θ_m.

Since $A_n \propto \sin \frac{\pi}{a} x_n \approx \frac{\pi}{a} x_n$, $g \propto A_n^2$, [4,5] and with the impedance matching requirement in design that, for a standing wave array, [5] $\sum_n g_n = 1$, it can be seen that $\sum_n \left| A_n x_n \right|$ or the strength of the second-order-beam is approximately constant, independent of the number of elements in the array.

For the array which was used in testing the range, and with $\left| 90^\circ - \phi \right| = 5^\circ$, that is, an error of 5° is made in positioning the array, then $k \sin \theta_m \cos 85^\circ \, e(\theta_m, 85^\circ) \sum_n \left| A_n x_n \right|$ is 39.2 db below $\sum_n A_n$, which is the amplitude of the main beam. Thus, a lobe of approximately this value would appear at $\theta \simeq \pm 44.5^\circ$ theoretically, since the design sidelobe near $\pm 44.5^\circ$ is -53 db and the sidelobe and the second-order beam are in quadrature. Based on the above analysis a curve showing the field strength of the second-order beam verus ϕ is shown in Figure 24.

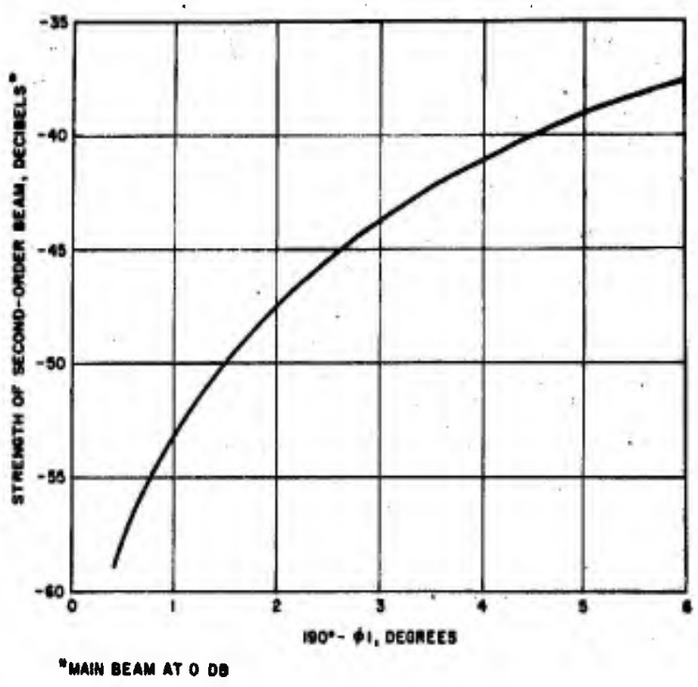

Figure 24.

As a by-product of this analysis, the direction of the second-order beam as a function of frequency at X-band is shown in Figure 25. At frequency 9.375 kmc, $\theta_m = 44.5^\circ$.

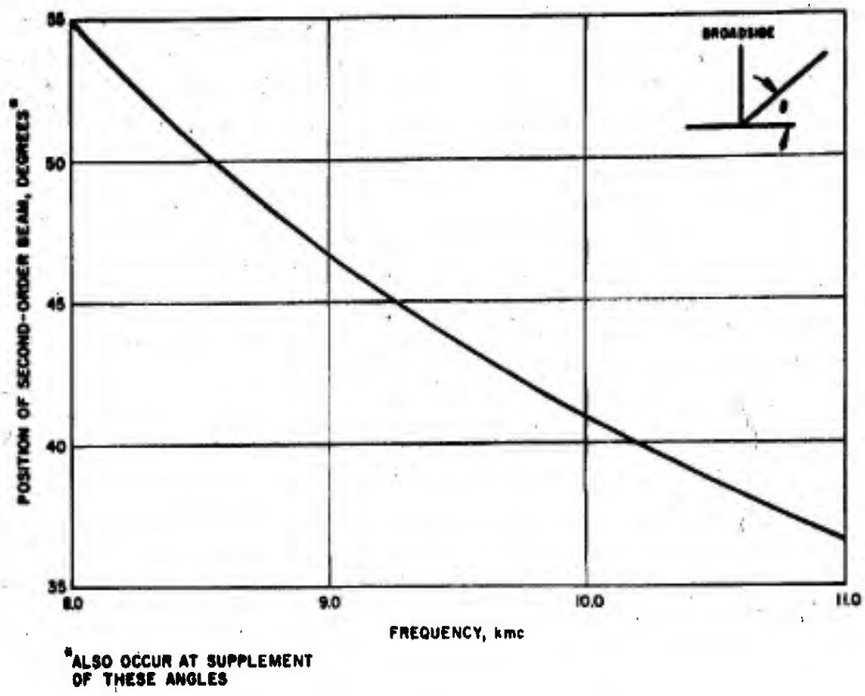

Figure 25.

SIMULTANEOUS SCAN TECHNIQUE

Certain antenna applications normally call for the use of conventional pencil-beam antennas which would either scan a desired angular region or obtain coverage by stacked-beam operation. Several well-known techniques are available for such scanning requirements but all possess certain shortcomings which make the development of new scanning methods mandatory. One such new technique is that known as simultaneous scan. This is an application of "time domain antenna techniques" in which by proper periodic modulation of the aperture excitation, the patterns at each resultant sideband frequency are beams pointing in different directions.

Theory

The basic technique of simultaneous scan may be outlined as follows. Consider a linear array of N equally spaced elements with a cw signal incident at an angle θ, measured from the array axis as shown in Figure 26.

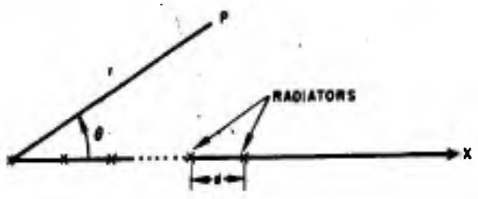

Figure 26. Array geometry.

All elements are identical and their separation is d. If each element is turned on and off in sequence so that as one is turned off the next one is turned on, and this is repeated periodically, the output from the array has the form (neglecting element factors)

$$f(\theta, t) = \exp(j\omega t) \sum_{p=-\infty}^{\infty} \sum_{m=0}^{N-1} \exp(j k m d \cos\theta) \left\{u[t - (m + pN)\tau] - u[t - (m + 1 + pN)\tau]\right\} \quad (31)$$

Here ω is the angular frequency of the incoming wave, and u(t) is the unit step function. This signal is a function which has phase discontinuities of kd cos θ every τ seconds and which repeat every Nτ seconds. These phase discontinuities are therefore measures of the angle of arrival of the signal. The angle of arrival information may be converted to a more conventional form by examining the spectrum of the signal. When the signal is written in terms of its spectral components it becomes

$$f(\theta, t) = \exp(j\omega t) \sum_{-\infty}^{\infty} f_n(\theta) \exp\left(j \frac{2n\pi}{N\tau} t\right) \quad (32a)$$

where

$$f_n(\theta) = \frac{1}{N\tau} \int_0^{N\tau} f(\theta, t) \exp\left[-j(\omega + \frac{2n\pi}{N\tau})\, t\right] dt$$

$$= \frac{1}{N} \exp(j \frac{n\pi}{N}) \frac{\sin \frac{n\pi}{N}}{\frac{n\pi}{N}} \exp\left[j \frac{N-1}{2} (kd\cos\theta - \frac{2\pi n}{N})\right]$$

$$\frac{\sin \frac{N}{2} (kd\cos\theta - \frac{2n\pi}{N})}{\sin \frac{1}{2} (kd\cos\theta - \frac{2n\pi}{N})} \qquad (32b)$$

Each $f_n(\theta)$ peaks for a different angle of arrival given by

$$\cos\theta_n = \frac{n\lambda}{Nd} \qquad (33)$$

It may also be seen that where one $f_n(\theta)$ has a peak all others are zero, and that adjacent frequency components correspond to spatial patterns with adjacent overlapping beams. Therefore, by filtering the various frequency components, continuous coverage of space is achieved. Figure 27 illustrates the coverage as a function of $u \equiv kd\cos\theta$. When $d = \lambda/2$, beams which scan from $\theta = 0$ to $\theta = \pi$ are obtained from sidebands in the range $-\frac{N}{2} \leq n \leq \frac{N}{2}$. Continuous observation of the $N + 1$ frequency components gives essentially continuous angle of arrival information.

Experimental Array

In accordance with the above theory a twenty-element simultaneously scanned array is under construction. The array consists of twenty X-band slot radiators, each fed through a separate branch guide from a common main feed guide. Each branch line will contain an on-off rf diode switch

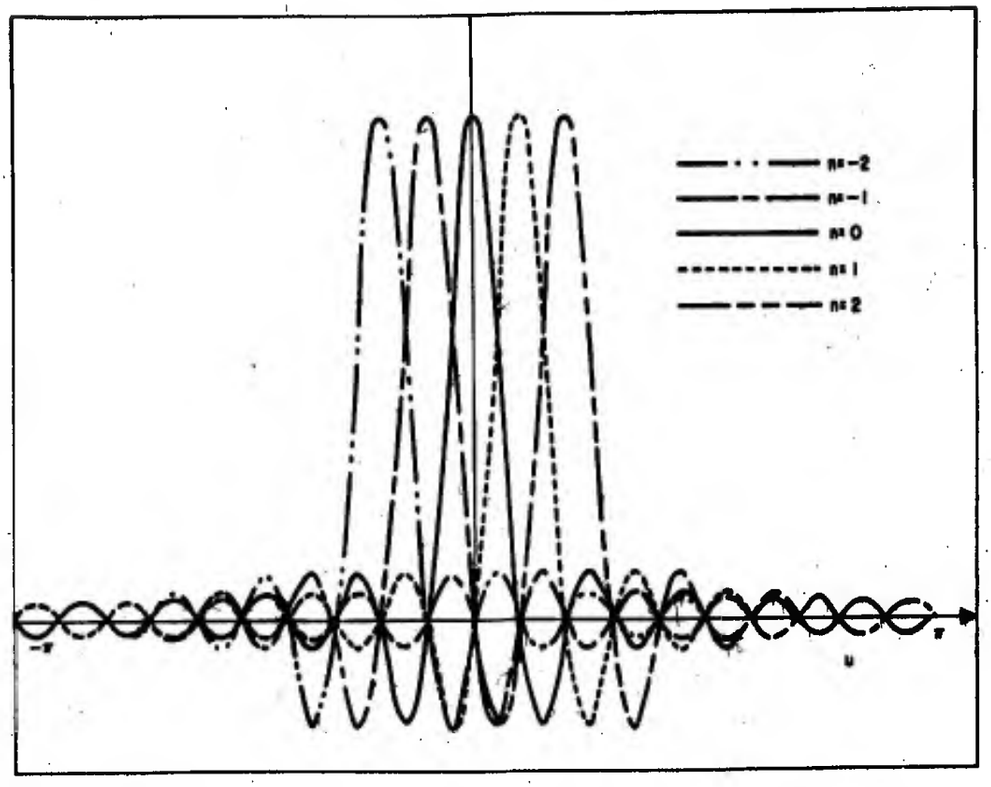

Figure 27. Illustration of coverage of five beams for 20 element simultaneously scanned array.

which will be controlled by a programming network to obtain the required sequential excitation of the array elements. For experimental purposes the fundamental modulation frequency of the array will be 10 kc and the sidebands will be detected by a special receiver which uses quadruple detection with the filtering done at an intermediate frequency of 250 kc. The basic receiver system has been outlined in this report in the section describing the transmitter and receiver.

The control circuitry for the array is now being developed. The array requires circuitry which will turn the rf switches on and off sequentially and repeat the entire sequence every 10^{-4} seconds. Since there are twenty switches, each switch is on for five microseconds during each period. For good operation the switching times must be a small fraction of a microsecond. Switching times of the order of one tenth of a microsecond are anticipated. The distribution of the switching pulses to the various switches will be accomplished with Burroughs Beam -X switching tubes. These tubes each have ten constant current output terminals which are sequentially turned on and off with successive input pulses. It is expected that obtaining proper operation of this switch driving circuitry will be the major source of difficulty in realizing satisfactory array performance.

Minimizing the effects of differences in individual rf switch characteristics may also present some problems. The differences may upset the resultant array aperture distribution. This can be overcome through the use of adjustable phase shifters and attenuators in each element feed line. However, this represents an additional equipment complexity which should be avoided if possible. The adjustments in the excitation of each element may have to be made independently so that uniform aperture illumination results for every pattern.

CONCLUSIONS

A design analysis has been presented for a linear array which obtains reduced sidelobe levels by on-off switching of the individual array elements and a simplified experimental array with its control circuitry have been described.

The required stable transmitter and receiver as well as filtering equipment necessary for obtaining proper time domain operation have been developed.

The final results of the pattern range testing indicate that it should be possible to measure 40 db sidelobes to within ±1.5 db.

The theory of simultaneous scan operation has been presented, and an experimental twenty-element array with its control circuitry is being developed.

REFERENCES

1. Bailin, L.L. and Erlich, M.J., "Factors Affecting the Performance of Linear Arrays," Proc. I.R.E. 41 (1953) pp. 235-241.

2. O'Neill, H.F. and Bailin, L.L., "Further Effects of Manufacturing Tolerances on the Performance of Linear Shunt Slot Arrays," I.R.E. Trans.-P.G.A.P. Vol. AP-4, December 1952, pp. 93-102.

3. Ramo, S. and Whinnery, J.R., Fields and Waves in Modern Radio, John Wiley and Sons, Inc., New York, 1953.

4. Stevenson, A.F., "Theory of Slots in Rectangular Waveguides," Journal of Applied Physics, Vol. 19, January 1948, pp. 24-38.

5. "Waveguide Slot Array Design," TM-348, Hughes Aircraft Company, July 1954.

6. "A Two-Parameter Family of Line Sources," TM-595, Hughes Aircraft Company, October 1956.

7. Gruenberg, H., "Second Order Beams of Slotted Waveguide Arrays," Can. J. Phys. Vol. 31, 1953, pp. 55-69.

UNCLASSIFIED